Design and modeling the spiral magnetic structure for 80 MeV H^- isochronous cyclotron

N.K.Abrossimov, S.A.Artamonov, V.A.Eliseev, G.A.Riabov

Petersburg Nuclear Physics Institute RAS, Russia

The magnetic structure with high spiral angle is applied for 80 Mev H^- isochronous cyclotron. This structure provides the highest possible energy of accelerated H^- ions for a given magnet under condition that beam losses due to electromagnetic dissociation is lower than 5%. The special methodology for approximate determination of hill and valley gaps, flutter and effect of spiraling on flutter with the aid of widely used 2D POISSON code is developed. Among another things the flutter is found to be dropped rapidly on the radii smaller than double hill gap. As a result the straight sectors with zero spiral angle has to be used in central region. The calculation results has been verified by the magnetic measurements on the models with scale $k_1 = 1.33$ and $k_2 = 8$. On the scale models effect of discrepancy between the spiral in the magnetic field and pole tips was investigated. This effect must be taken into account under design the magnetic structure with high spiral angle.

1 Introduction

The design and construction of the 75-80 MeV H^- cyclotron is being in progress at PNPI [1]. To reduce the expenditure the cyclotron magnet has been designed to use the iron of the model magnet of the operating 1 GeV synchrocyclotron.

The cyclotron magnetic field must meet some requirements. The magnetic rigidity on the final orbit must achieve Br = 13.2 kGs·m that corresponds to the 80 MeV energy. For isochronism it must be provided 8.5 % increasing of the azimuthally averaged magnetic field from center to final orbit. The azimuthal variation of the magnetic field must provide for z-focusing and permissible value of vertical oscillation frequency ν_z. Room has been left for the high frequency system and the gap between shims must be more than 140-150 mm. For H^- cyclotron there is an additional and essential requirement connected with confining the electromagnetic dissociation of H^- ions in the limit of 5 %.

There are two main problems connected with design the magnetic field of isochronous cyclotron. The first one is the selection of the magnetic structure provided the highest possible energy of the accelerated H^- ions for a given magnet under condition that beam losses is lower than 5 %. The next problem is determination of the pole tips geometry which provides the selected field structure.

2 H^- losses and selection of the magnetic structure

The H^- losses due to electromagnetic dissociation are defined by the ion energy and magnetic field. In our case the final radius of acceleration is fixed and the final acceleration energy W_{max} defines $\bar{B}(r_f)$. In this case the maximum field in cyclotron can be reduced only by using the magnetic structure with low magnetic field in the hill. The needed focusing must be provided by using of the high value of the spiral angle.

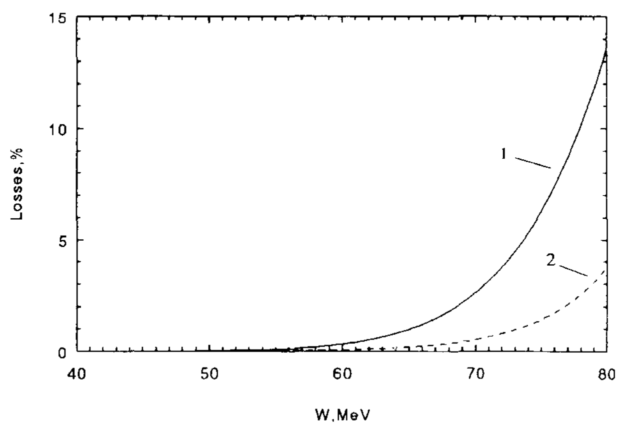

Figure 1: H^- losses due to electromagnetic dissociation for two magnetic structures.

Numerical calculations results of the life-time and beam losses for the cyclotron at Gatchina [2] with the input parameters $r_f = 0.9$ m, $\bar{B}(r_f) = 14.67$ kGs, $B_0 = 13.52$ kGs, and $N = 4$ can be formulated as follows.

- The main beam losses of H^- ions on the electromagnetic dissociation takes place in hills region, where the life-time $\tau \sim 100$ times less than in valley.
- For energy gain $\sim$ 200 keV / turn the life-time becomes comparable to the acceleration time ($\sim 10^{-5}$ sec.) under energy more high than 60 MeV.
- Two alternative versions of the magnetic structure have been examined. The first one (1) have on the final radius flutter $F = 0.04$, spiral angle $\gamma = 55^o$, harmonic amplitude $A_4 = 4.15$ kGs and second structure (2) with $F = 0.025$, $\gamma = 65^o$, $A_4 = 3.28$ kGs. As it

is well known, γ is an angle between the radius vector at radius r and tangent to the median line of sectors at the same radius.

The both modifications provide about the same net axial focusing and are distinguished by the field in the hill region. In the Fig.1 are presented the beam losses due to electromagnetic dissociation for two versions of the magnetic structures. The second version—with low flutter and high spiral angle was selected for Gatchina cyclotron as a provided beam losses lower than 5%.

3 The magnet design and optimization

Next problem is connected with the determination the shape of the pole tips which provides the needed magnetic field distribution.

Approximation of the uniform magnetization. The sector focusing properties have been examined in the set of reports [3,4] in the approximation of the uniform magnetization. In [3] is obtained the expression for the main Fourrier component of the magnetic field variation for the infinity series of the rectangular bars disposed symmetric about the median plane

$$B_N = 8M \sin(\frac{2\pi a}{d}) \exp(-\frac{2\pi g_h}{d}),$$

where $2a$–bar width, $2g_h$– gap between the bars, d–structure period equal to the total width of the hill and valley, $4\pi M = 21kGs$.

For the case of isochronous cyclotron $d = 2\pi r/N$, where N–number of sectors, the flutter increases with the radius

$$F \sim \frac{B_N{}^2}{2} \sim \exp(-2/x),$$

where $x = r/Ng_h$.

Although the accuracy of this approximation is inadequate to give the quantitative results (see Fig.3), this model makes possible to introduce some useful parameter like x and give the general idea of the relations between the structure parameters. In particular, nondimensional scale parameter $x = r/Ng$ allow to compare the different structures. For $x < 0.5$ the flutter is very low and increases with the growing x, the lower gap g_h and number of sectors N the higher the flutter. The maximum value of the field harmonic and flutter corresponds to equal lengths of the sector and valley, when $a = 0.25d$ and $\sin(\pi/2) = 1$.

Selection of the final radius and gaps. The model magnet had the following characteristics: diameter of the cone poles equal to 1.5 m; gap equal to 289 mm; nominal excitation current equal to 1.2 kA. The modernization of the magnet has been based on the calculation using 2D code POISSON [5]. In order to decrease the magnetic field on the final orbits at given Br the diameter of the pole has been increased up to 2 m. The calculations have showed that $\sim$ 30% increasing of the pole radius from 0.75 m to 1 m causes the increasing of the magnetic flow up to more than 1.6 times and causes saturation of the pole iron. Therefore the cross section of the yoke has been increased by 16% and the height of the side pillar decreased by 0.5 m. These procedures allowed decrease the maximum field in the magnet yoke down to 23.5 kGs, decrease the excitation current down to 800 A and reduce power consumption down to 120 kW.

The base problem under the design the cyclotron magnet is a selection the averaged gap, excitation current and also the hill and valley gaps. Set of the axially symmetrical magnets has been calculated with the averaged gaps $2g_0$ = 260, 300 and 360 mm, with the corresponding set of excitation currents and the ring shims which provided the same $\bar{B}(r)$ corresponding the isochronous magnetic field for 80 MeV energy at the radius r_f = 0.9 m. From these calculations it was estimated also that 1 cm thickness of shim on the last ring corresponds to the field $\sim$ 1 kGs. In this a case the 8 kGs variation of the field corresponds about 8 cm step in the iron height as one passes from valley to hill. On the base of the above consideration variant with average gap 300 mm has been selected. That variant provides isochronous field and the minimum gap of hill $\sim$ 150 mm and valley gap $\sim$ 380 mm.

The final shim profile is shown in Fig.2. To ease of manufacture the hill shimm height is selected a constant along the radius and to keep isochronism same amount of iron was cut in the valley central region.

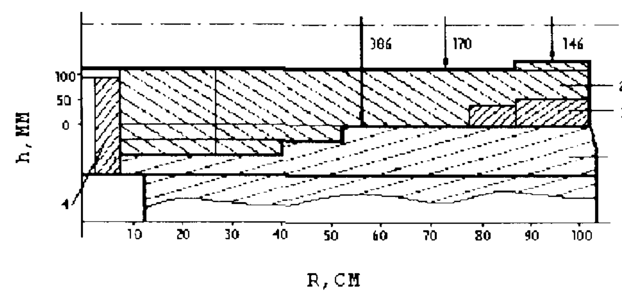

Figure 2: Shim profile in the hill and valley: 1–pole tip, 2–sector, 3–valley's shim, 4–central plug.

Flutter as a parameter having been determined by the azimuthal magnetic field distribution can not be exactly calculated by 2D code. However it is developed [6] the approximative methods of the estimation the flutter for the straight sectors if the azimuthal edge effect is represented as radial one. The results of calculation for two different thicknesses h_i of the sector iron and two sets of hill and valley gaps $2g_h$ and $2g_v$ respectively are presented in Fig.3.

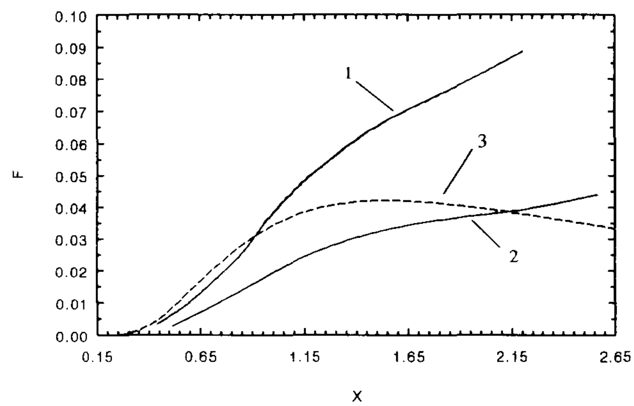

Figure 3: Flutter in dependence on nondimensional parameter $x = r/Ng_h$, where $N = 4$, 1–$2g_v$ = 386 mm, $2g_h$ = 170 mm, h_1 = 108 mm; 2–$2g_v$ = 284 mm, $2g_h$ = 145 mm, h_2 = 69 mm; 3–uniform magnetization for the case 1.

Effect of spiral pole tips. Spiraling of pole tips introduces alternating gradient components which increase the net focusing. The effective value of the flutter in such a case is multiplied by the factor $S(r,\gamma) = 1 + 2\tan^2\gamma(r)$. However the actual gain in focusing is less than that expected due to two effects:

- discrepancy between the spiral angle of field and pole tips due to edge effect (see in more details item 4);
- flutter falling as the spiral is introduced because the distance between the sectors along the perpendicular to median line of sector is reduced what is the same as decreasing the structure period.

According to the simple geometrical consideration [7] effective reduction in the structure period can be expressed as $d_{eff} = d cos\gamma$.

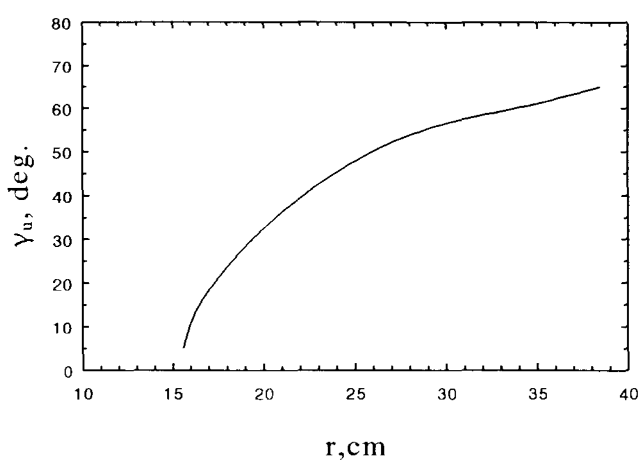

Figure 4: The ultimate spiral angle on dependence of radius for $2g_v = 386mm, 2g_h = 170mm, r = Ng_h x_{eff}$, $N = 4$.

As a result the effect of the flutter falling can be obtained from data presented in Fig.3 if instead of x to substitute effective value $x_{eff} = x\cos\gamma$. The overall effect of the spiraling can be expressed by the parameter which is product of two multiplicand: flutter F and $S(r,\gamma)$. As $x_{eff} < 0.5$ flutter is drastic decreased this can cause the reduction of focusing. The ultimate spiral angle for every value of parameter x can be found as a root of the equation

$$U(x,\gamma) = (F(x\cos\gamma)/F(x)) \cdot (1 + 2\tan^2\gamma) - 1 = 0,$$

where $F(x)$ is a function shown in Fig.3. In the Fig.4 is shown the ultimate spiral angle on dependence of radius. As illustrated in Fig.4 the spiraling is ineffective on the radii smaller than 15 cm and the high spiral angle is reasonable to use only for radii $r > 35$ cm.

4 Measurements on the models

In parallel with the numerical calculations the experimental measurements on the scale models have been performed for the direct investigation of 3D effects and verification of the admitted approaches.

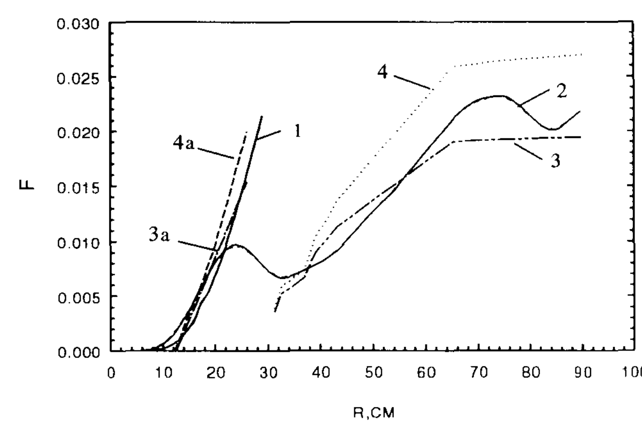

Figure 5: Flutter in dependence on cyclotron radius: 1 — the data of the measurements on model with straight sectors k_1 = 1.36 (central part); 2 — the data of measurements on model with high spirallity k_2 = 8; 3 — calculations on the base of proposed methodology with $2g_v$ = 284 mm, h_1 = 69 mm; 4 — calculations with $2g_v$ = 386 mm, h_1 = 108 mm; 3a, 4a — calculations with straight sectors.

Two models with the scales $k_1 = 1.33$ and $k_2 = 8$ and spiral angles $\gamma_1 = 55^o$ and $\gamma_2 = 65^o$ respectively have been examined. The model variants have the same azimuthal sector extension and sector thickness. Two models with different spiral angles give the same average magnetic field and the measurements and calculation are in good agreement. In Fig.5 is shown the dependence of the flutter on radius for the calculation and experimental results.

Calculation for the models with high spiral angle are performed on the base of Fig.3 with the use methodology of $x_{eff} = x cos\gamma$. Proposed methodology presents a way of estimation the flutter with acceptable accuracy. On the models were investigated also the discrepancy in behavior between the phases of the field harmonic and the sector median line along radius. In Fig.6 are presented phase of the main harmonic and the azimuth of median line of the sector iron along radius for model $k_2 = 8$.

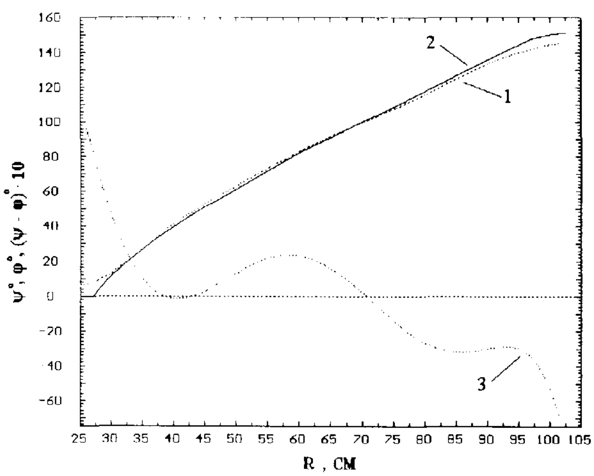

Figure 6: ψ (1) is phase of the main harmonic and φ (2) is a median line of iron sector along radius,($\psi - \varphi$) (3) is phase discrepancy along the radius.

In Fig.7 are shown the geometry spiral angle as well as corresponding to it magnetic spiral angle.

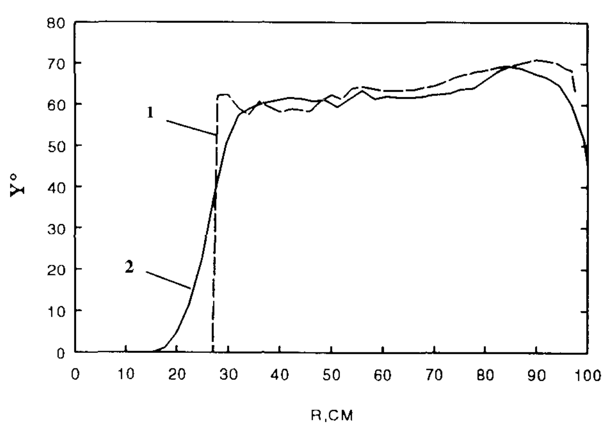

Figure 7: Spiral angle in dependence on cyclotron radius: 1 - geometry data of k_2=8 model; 2 experimental values.

The discrepancy between effective and geometrical spiral angles reach 4^o that at 65^o corresponds to 30% focusing reduction by comparison with the sector iron geometry and this effect must be taken into account under magnet design. This effect was described in [4] and on the last radii can be explained by edge effect as magnetic field breaks away from the sector iron spiraling.

5 Conclusion

The magnetic structure with high spiral angle provides the final energy 80 MeV for the 2m diameter magnet and beam losses due to electromagnetic dissociation is lower than 5%. The magnet design and optimization was made by using of widely distributed 2D code POISSON. It was developed method of calculation the effect of the flutter falling as the spiral is introduced. As a result spiraling of pole tips increases the net focusing only on radii more than some ultimate one (see Fig.4) and in the central region the straight sectors have to be used.

The main calculation results have been verified by the experimental measurements on the scale model magnets. On the models was investigated effect of reduction the focusing due to discrepancy between magnetic field and pole tips spiral angles. In our case the focusing reduction can reach 30% and this effect must be taken into account under magnet design.

By now magnet of the isochronous cyclotron at Gatchina is fully manufactured including the spiral sectors and assembled. The test magnetic measurement of the excitation curve has shown that there is a good agreements between the models, calculations and full scale magnet.

References

1. N.K. Abrossimov et al., *Proc. XIII Intern. Conf. on Cycl. and their Applic.*, Vancouver, Canada,58 (1992).
2. N.K. Abrossimov, S.A. Artamonov, V.A. Eliseev, G.A.Riabov, *Preprint PNPI-2146*, Gatchina (1997).
3. V.I.Danilov,*Preprint JINR-R-409*, Dubna (1959).
4. H.G.Blosser and D.A.Jonson, *NIM*,**121**,301 (1974).
5. F.C.Iselin,*CAS*, Geneva, 181 (1987).
6. P.Heikkinen, *NIM in Physics Research* ,**A301**, 417 (1991).
7. N.K. Abrossimov, S.A. Artamonov, V.A. Eliseev, G.A.Riabov, *Preprint PNPI-2049*, Gatchina (1995).